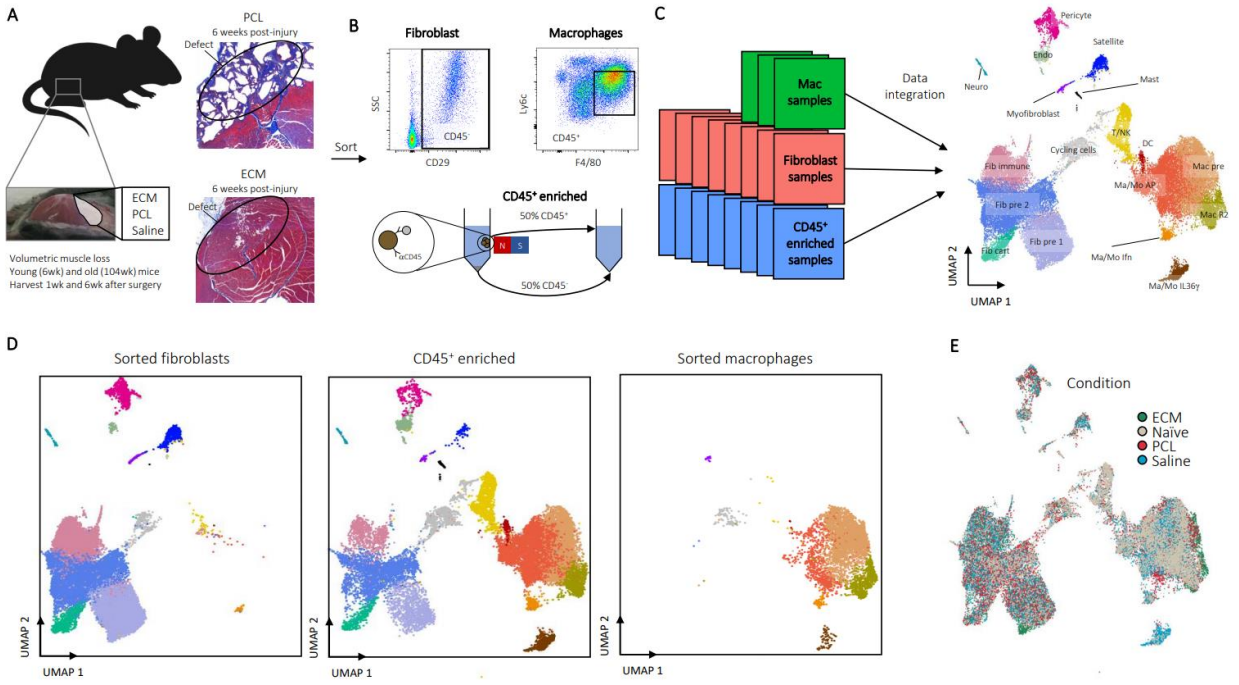

Supplementary Figure 1: Experimental Overview of Assembled Data Sets.
A, All data sets were taken from mice after volumetric muscle loss treatment. After surgical excision of a large portion of the quadriceps, the wound site was filled with a biomaterial or saline control and stapled shut. Mice were then harvested 1 or 6 weeks after surgery. Young (6 week) or aged (104 week) old animals were used. Representative histological images of PCL and ECM treated muscles 6 week after injury are shown stained by Masson's Trichrome. Muscle fibers are stained red and connective tissue is stained blue. The posterior (P) is labeled and the location of original defects circled. **B**, At time of harvest, cells were isolated one of three ways after digestions. For macrophages, cells were sorted as $CD45^{+}F4/80^{Hi}Ly6c^{+}$, for fibroblasts cells were sorted as $CD45^{-}CD19^{-}CD29^{+}$, and for the all-cell dataset $CD45^{+}$ cells were enriched to ~50% using MACS beads. **C**, Data sets were integrated for analysis using Harmony. A complete summary of available data sets is given in Supplementary Table 2. **D**, Enrichment of fibroblasts and macrophages due to inclusion of sorted fibroblast and macrophage data sets. The sorted fibroblasts (left) and macrophages (right) are shown in comparison to the $CD45^{+}$ enriched sample (middle). **E**, Cells by condition. Cells are colored by condition plotted on UMAP dimensions. Cells were plotted in order of ECM, PCL, Saline, and Naïve.

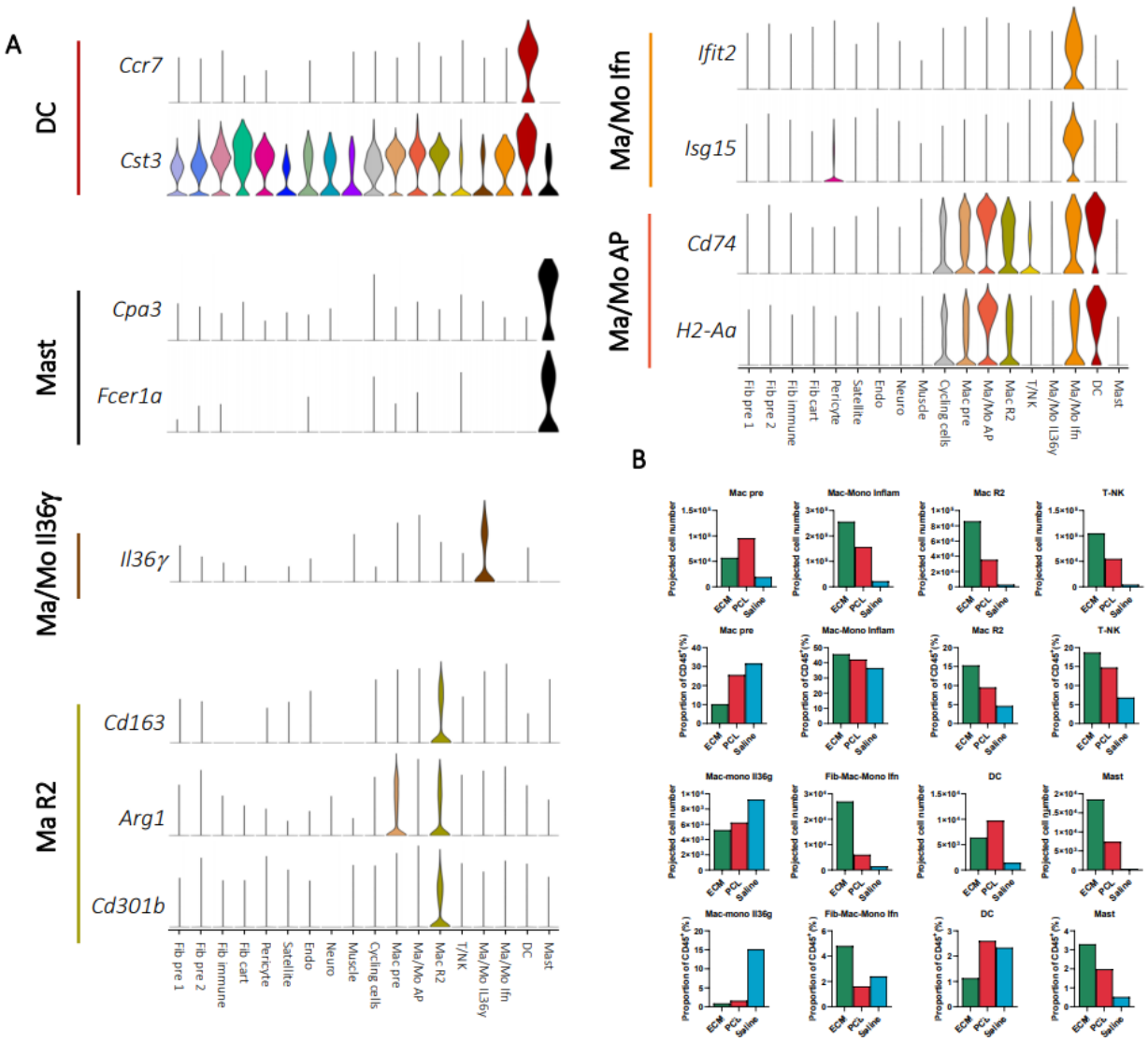

Supplementary Figure 2: CD45⁺ cluster expression characteristics and comparison with flow cytometry.

A, Gene expression for myeloid cluster markers. Single cell gene expression for marker genes used to identify myeloid clusters in tandem with CD14, CD11b, and F4/80 expression are shown as violin plots. **B**, Comparison of flow cytometry cell proportions to single cell proportions. Myeloid ($CD45^+CD11b^+$) and T cell ($CD45^+CD3^+$) numbers by flow cytometry given as raw counts (top left) and percent of the $CD45^+$ population (top right) from ECM, PCL, or saline treated animals. Mean values are plotted with standard error shown on error bars. $CD45^-$ and $CD45^+$ count values are shown, which were used to project single cell proportions to predicted raw numbers. Project single cell counts are shown by cluster (middle) by multipltying raw $CD45^+$ and $CD45^-$ counts from flow cytometry with cluster proportions of $CD45^+$ or $CD45^-$ populations from single cell (bottom).

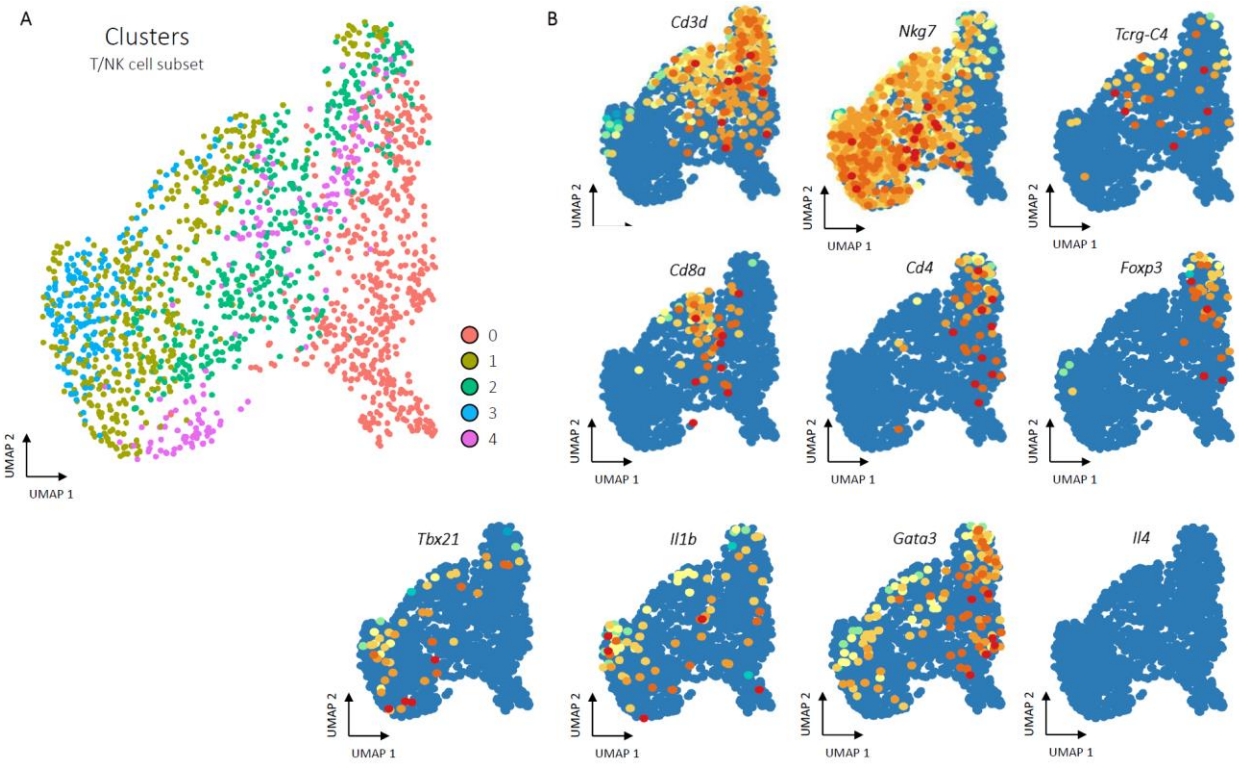

Supplementary Figure 3: Subset clustering of T/NK cells.
A, Clustering of T/NK cells. After subsetting to only T/NK cells, principle component analysis, clustering, and UMAP was run following the same procedures as the whole dataset. The five resulting clusters are visualized in the T/NK cell specific UMAP space. **B**, Gene expression for T and NK cell markers.

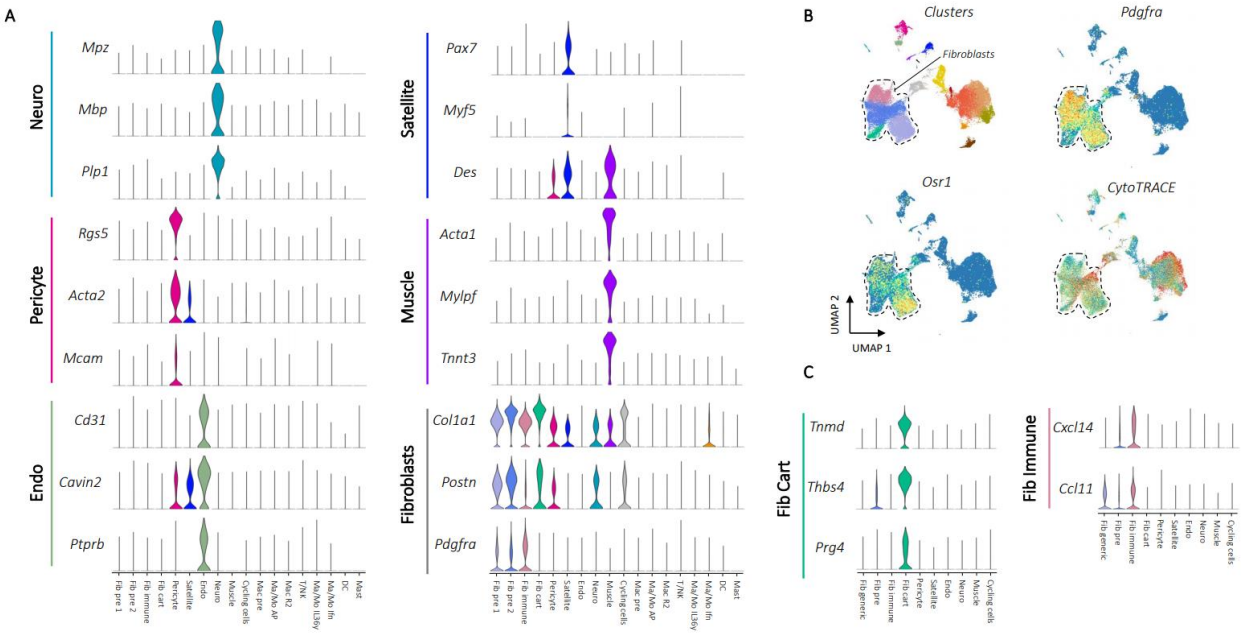

Supplementary Figure 4: CD45^{-} cluster expression characteristics.
A, Marker gene expression for non-fibroblast CD45- cell populations. Up to three characteristic gene markers are shown for each cluster by violin plot of normalized gene expression data. Fibroblast markers were used to identify the four fibroblast clusters Fib pre 1, Fib pre 2, Fib immune, and Fib cart. **B**, Stemness markers for fibroblasts. *Pdgfra* expression and clusters are shown to demonstrate location of fibroblasts with a dotted line drawn surrounding the fibroblasts. Stem marker *Osr1* and CytoTRACE score, an algorithm used to score cells for stemness, is shown below. **C**, Expression of characteristic markers for the tenocyte-like and immune fibroblast clusters.

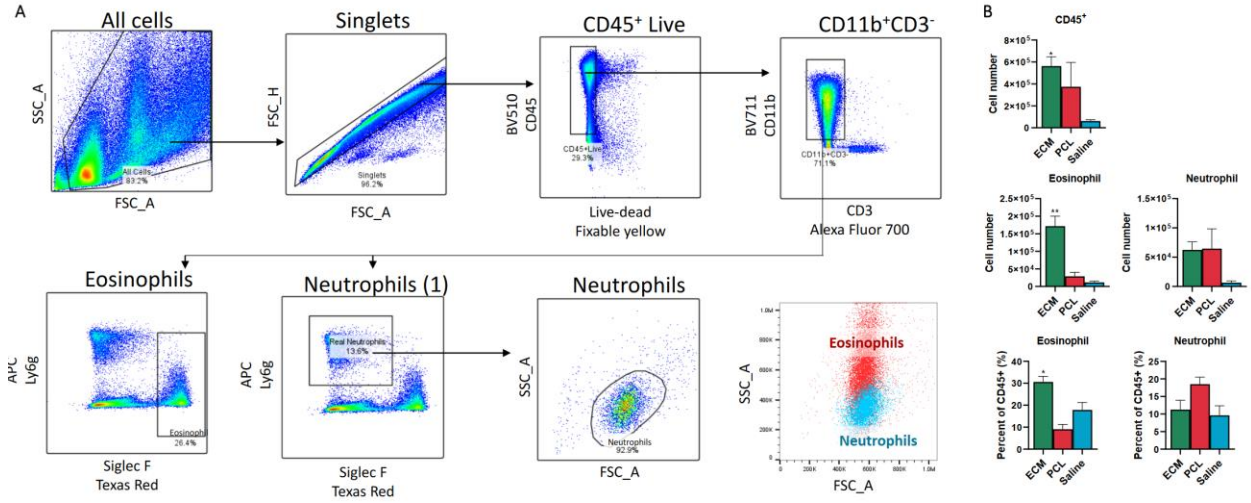

Supplementary Figure 5: Flow cytometry of neutrophils and eosinophils.
A, Cells were gated on scatter (FSC_A, SSC_A) followed by doublet discrimination (FSC_A, FSC_H), selection of CD45$^+$ live cells (Fixable Yellow-, CD45+), and selection of myeloid cells (CD3-, CD11b+). This population was used to identify eosinophils (Ly6g low, Siglec F+) and neutrophils (Ly6g+, Siglec F-) of correct size (FSC_A, SSC_A). **B**, Numbers of CD45$^+$ cells, eosinophils, and neutrophils from ECM, PCL, or saline treated animals one week after surgery (top). Eosinophil and neutrophil amounts as proportion of CD45$^+$ cells are given below. Data are mean ± SEM. $^{**}P < 0.01$, $^{*}P < 0.05$ by analysis of variance (ANOVA) followed by Dunnett's multiple comparison testing where *P* is adjusted p value.

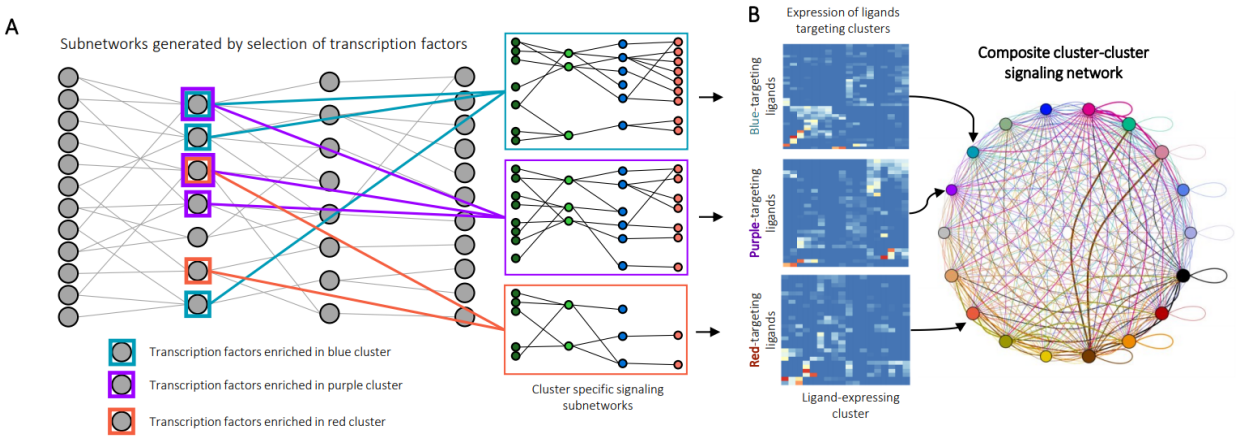

Supplementary Figure 6: Identification of intercluster signaling with Domino
A, Identification of cluster-specific signaling subnetworks. Transcription factors enriched by cluster are identified by Wilcoxon rank sum and networks pruned for disconnected nodes to generate signaling subnetworks relevant for biological activation of clusters. **B**, Calculation of intercluster signaling networks. Once phenotypically relevant receptors are identified by cluster specific signaling subnetworks, cluster-cluster signaling scores are calculated by cluster averaged scaled expression of ligands present in cluster-specific subnetworks. Every potential cluster-cluster combination is scored, and these weights used to generate an intercluster signaling network.

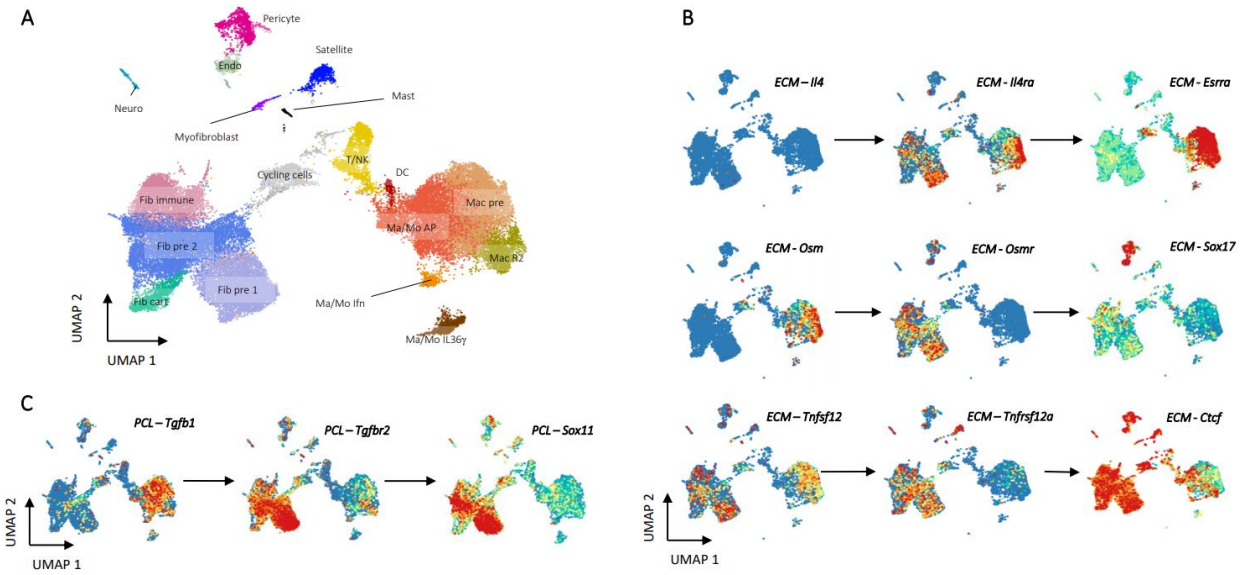

Supplementary Figure 7: Signaling pathways for ECM and PCL treated cells visualized with their known ligands.

A, A UMAP plot with clusters labeled for reference when viewing feature plots. **B**, ECM specific signaling pathways specified in Figure 3. Each pathway contains gene expression of ligands and receptors from each pathway, as well as transcription factor activation scores for the predicted transcription factor target. Ligands completely absent from the data set are not shown, although they may still be viable targets for a target receptor. **C**, PCL specific signaling pathways specified in Figure 3. No readily accepted ligands for *Pirb* have been identified, so the *Pirb Irf4* pathway is not shown.

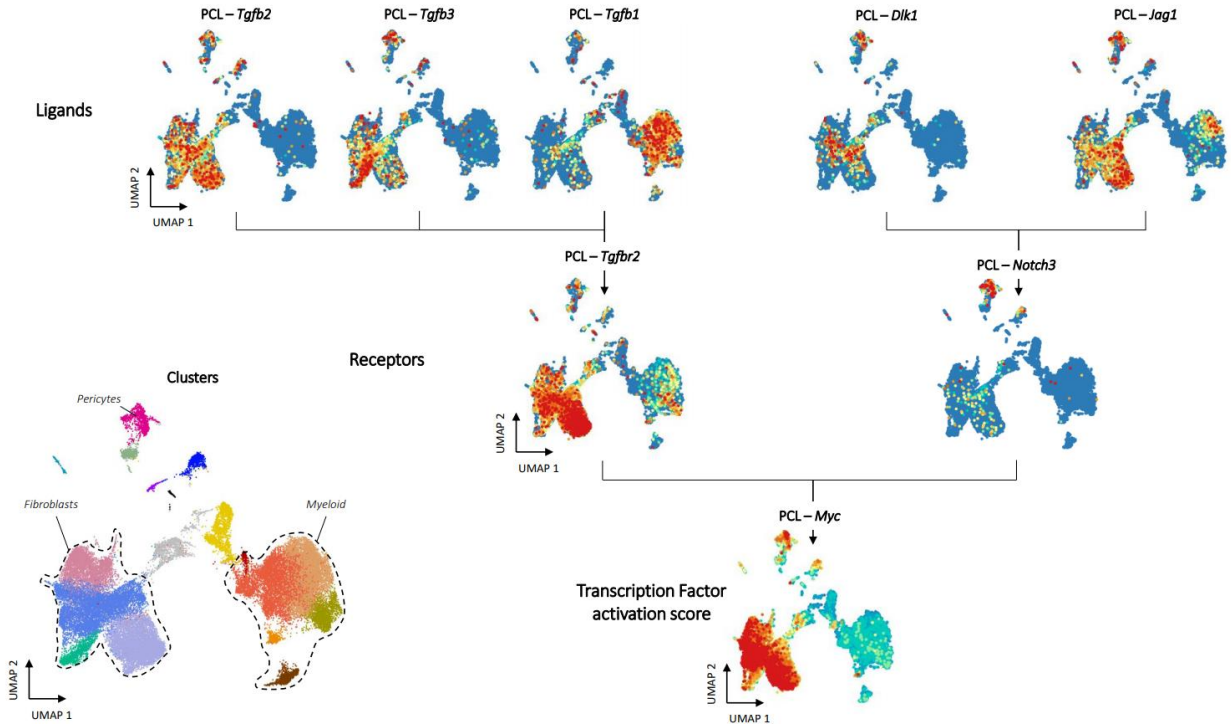

Supplementary Figure 8: Myc signaling in the PCL treated wound.
Gene expression of ligands and receptors predicted to be involved in activation of Myc in the PCL Domino signaling network for cells from PCL treated animals (top and middle). Myc expression values are SCENIC transcription factor activation scores (bottom). A reference of clusters is provided in the bottom left.

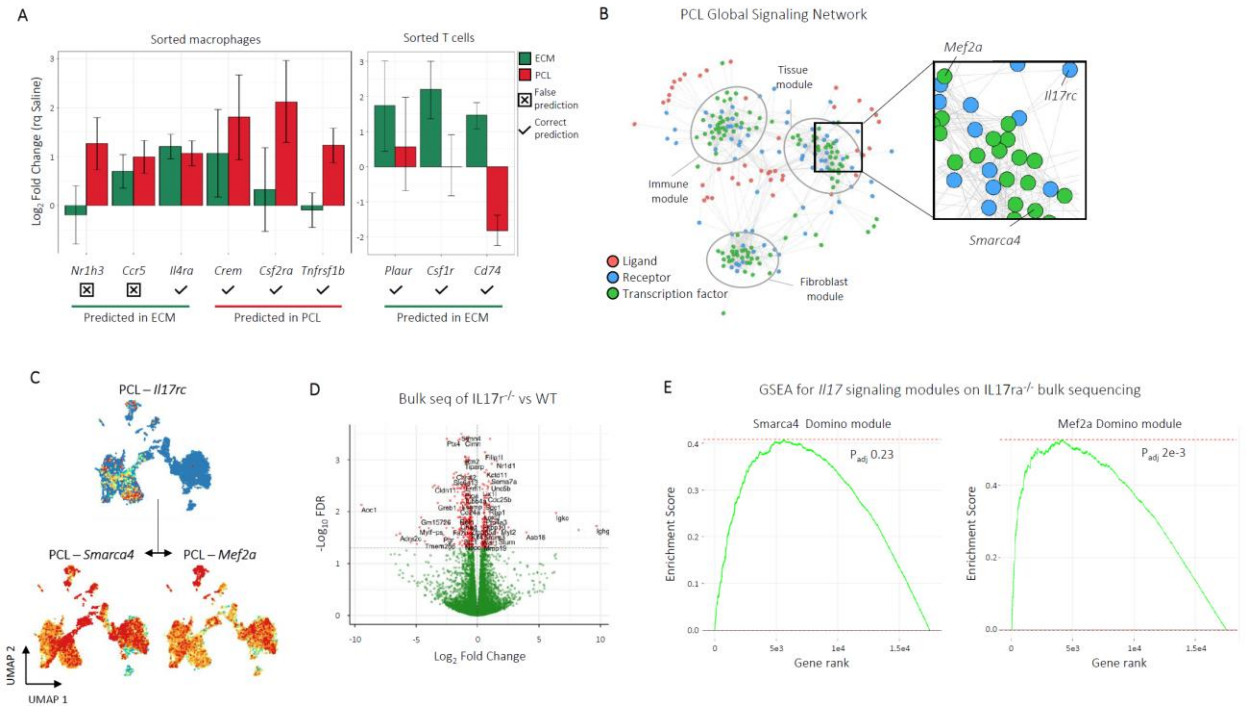

Supplementary Figure 9: *In vivo* validation of Domino signaling predictions.
A, Nanostring gene expression profiling for receptors and transcription factors identified as enriched in either ECM or PCL for specific cell types. After identifying genes specific to either ECM or PCL within the myeloid or T cell populations in Domino, we used Nanostring to probe expression of those genes in sorted myeloid ($CD45^+CD11b^+$) or T cells ($CD45^+CD3^+$). Of the 9 genes found to overlap between Domino and Nanostring, 7 were predicted correctly and 2 incorrectly. Error bars are standard error of the fold change estimate according to nCounter© software output. **B**, The Domino global signaling network for PCL as seen in Figure 5. The region surrounding the IL17 signaling pathway is enlarged and the components labeled. **C,** Expression of *Il17rc* and activation of it's predicted transcription factor targets *Smarca4* and *Mef2a* in the PCL signaling network. **D**, Volcano plot for bulk RNA sequencing of $IL17ra^{-/-}$ and wild type animals one week after VML. Direction of log fold change indicates expression in $IL17ra^{-/-}$ animals compared to wild type. An FDR threshold of 0.05 was used to designate genes as significant. **E**, Gene set enrichment analysis (GSEA) of Domino transcription factor modules predicted as downstream of IL17 in the PCL signaling network. Both modules predicted to interact are shown. Genes from the edgeR bulk RNA seq comparison with respect to wild type ordered by FDR were used to calculate enrichment for genes present in the Domino transcription factor modules. Movement of the running enrichment score (green line) above zero indicates enrichment of genes in the module in the statistically significant portion of expressed genes while movement below zero indicates enrichment of genes in the module in the lower FDR portion of the genes. P values calculated by GSEA adjusted by Benjamini-Hochberg correction are shown.

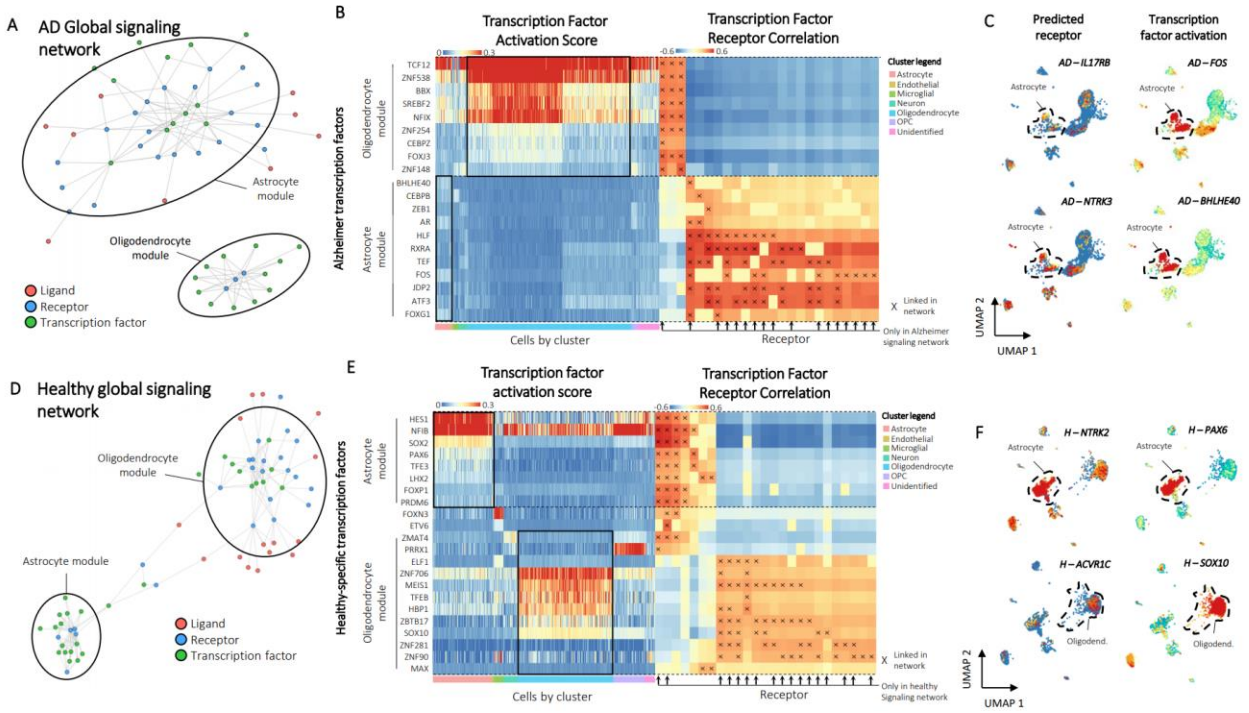

Supplementary Figure 10: Pathological signaling found from a public dataset of Alzheimer's Disease.

A, The Alzheimer's disease (AD) global signaling network. two modules of receptors and transcription factors are readily apparent and labeled based on enrichment of transcription factors by cluster. **B**, Heatmaps of transcription factor activation score for AD-specific transcription factors (left) and correlation of transcription factor activation score with receptor expression (right). Transcription factors are binned according to their membership to the astrocyte or oligodendrocyte modules from the AD global signaling network. Cells are ordered and colored according to their cluster. Receptors found only in AD are marked with arrows. Connections between receptor and transcription factors are marked with an 'x' on the correlation heatmap. **C**, Example feature plots of gene expression and activation scores for specific receptor-transcription factor pairs identified by domino in the AD condition. **D**, The healthy global signaling network. Two modules of receptors and transcription factors are readily apparent and labeled based on enrichment of transcription factors by cluster. **E**, Heatmaps of transcription factor activation score for healthy-specific transcription factors (left) and correlation of transcription factor activation score with receptor expression (right). Transcription factors are binned according to their membership to the astrocyte or oligodendrocyte modules from the global signaling network. Cells are ordered and colored according to their cluster. Receptors found only in the healthy signaling network are marked with arrows. Connections between receptor and transcription factors are marked with an 'x' on the correlation heatmap. **F**, Example feature plots of gene expression and activation scores for specific receptor-transcription factor pairs identified by domino in healthy cells.